

## PITYOSTROBUS ANDRAEI (PINACEAE) FROM THE BARREMIAN (LOWER CRETACEOUS) OF BELGIUM: A MORPHOMETRIC REVISION

Léa De Brito<sup>1,\*</sup> and Cyrille Prestianni\*

\*Evolution and Diversity Dynamics Lab, Université de Liège, Quartier Agora, Allée du Six Août, 14, 4000 Liège, Belgium,  
and Royal Belgian Institute of Natural Sciences, Rue Vautier 29, 1000 Brussels, Belgium

Editor: Alexandru M.F. Tomescu

Important floristic changes took place during the Early Cretaceous (145.0–100.5 Ma). They are notably marked by a peak in conifer diversity, especially within Pinaceae. This diversification is attested to by the numerous ovulate cone taxa found in the western European and North American fossil records. Exceptional deposits in the Wealden facies (Barremian-Albian, 125.0–100.5 Ma) of western Belgium (La Louvière, Houdeng-Aimeries) have yielded hundreds of exceptionally well-preserved pinaceous ovulate cones, yet most of these remain unstudied. These are presently revised. We investigate the morphological variation of the most abundant species, *Pityostrobus andraei* (Coemans) Seward 1919, with a morphometric approach. This work applies statistical tests to a large sample ( $n = 132$  fossil cones) for the first time, using 10 measurements to characterize the morphology of the cones. Our analyses recover eight distinct morphotypes included in the original specific concept of *P. andraei*, and most of the specimens belong to two main morphotypes that represent 50% and 25% of the total specimens analyzed. Our results suggest that the specific diversity of early Pinaceae is underestimated, as it is based on older species concepts. Modern quantitative approaches have the potential to better characterize the breadth and tempo of pinaceous diversification.

**Keywords:** Wealden, conifers, disparity, cone, morphometry, diversity.

**Online enhancements:** appendixes.

### Introduction

During most of the Mesozoic era (252.6–66.0 Ma), continental ecosystems were dominated by Cycadales, Bennettitales, and ferns. The Lower Cretaceous (145.0–100.5 Ma) was, however, marked by important floristic changes (Watkins and Cardelus 2012). Conifers that appeared in the Pennsylvanian (323.2–289.9 Ma) were expanding rapidly, increasingly colonizing the Northern Hemisphere continents, especially western Europe and North America (Bonnot et al. 1963; Miller 1977; Taylor et al. 2009; Smith et al. 2017). Some modern families, such as the Cupressaceae and Araucariaceae, were already present at the end of the Jurassic (Taylor et al. 2009; Herrera et al. 2017).

Among living conifers, Pinaceae have a wide ecological range, thriving in continental, mountainous, or subarctic environments (Bonnot et al. 1963; Critchfield and Little 1966; Smith et al. 2017). With 11 genera and about 230 species of trees and shrubs, it is the most diverse conifer family at the species level (Falcon-Lang et al. 2016; Gernandt et al. 2016). In the fossil record, Pinaceae are first found at the end of the Jurassic (*Eathiestrobus mackenziei*; Rothwell et al. 2012) and at the beginning of the Cretaceous (Valanginian, 140–133 Ma; Klymiuk and Stockey

2012; Falcon-Lang et al. 2016). Cones that are morphologically close to current pinaceous cones classified in modern genera such as *Pinus* (found in Belgium and England) appeared as soon as the Early Cretaceous (Alvin 1953, 1960; Ryberg et al. 2012; Falcon-Lang et al. 2016; Smith et al. 2017). The Pinaceae reached their maximal morphological disparity at about the same time (Oyston et al. 2016).

Our understanding of the early evolution and diversification patterns of Pinaceae is mainly based on isolated ovulate cones found in the Cretaceous and the Paleogene of Eurasia and North America (Gernandt et al. 2016). Consequently, as of now there are no studies that have quantitatively examined the inter- and intraspecific variability of these fossil cones. Taxonomic resolution for the form genus *Pityostrobus*, erected to encompass isolated pinaceous ovulate cones, is thus likely to be improved by further analyses intended to survey morphological data (Miller 1976; Ryberg et al. 2012). Weakly phylogenetically supported and with no clear diagnosis, *Pityostrobus* certainly does not form a clade (Smith et al. 2017). It nevertheless represents the most abundant Pinaceae form genus in the Lower Cretaceous, with 28 species of 42 pinaceous cones known for that interval (i.e., two-thirds of the species). Because of the large number of species included in it, this genus is responsible for major biases in phylogenies (Gernandt et al. 2016; Smith et al. 2017).

Descriptions of seed cone morphotaxa are subject to several inherent identification biases: quality of preservation, number of specimens available, and subjectivity of identification, depending

<sup>1</sup> Author for correspondence; email: l.debrito@uliege.be.

on the author. From a taxonomic point of view, *Pityostrobus* is a “dustbin” genus that encompasses multiple different species concepts. A standardization of the genus is needed to clarify the identifications of Pinaceae morphospecies and to develop reproducible methods of analysis for fossil ovulate cones. To this end, we tested the combination of descriptions and quantitative analyses presented here.

The current research was triggered by the reinvestigation of the Wealden collections housed at the Royal Belgian Institute of Natural Sciences (RBINS; Brussels, Belgium). At the end of the nineteenth century, several excavations in the Belgian Wealden (Lower Cretaceous) continental facies yielded hundreds of exceptionally well-preserved ovulate cones. Nine species have been described based on this material, and most of them have been included in comparative and phylogenetic studies of fossil and extant Pinaceae on multiple occasions (Smith and Stockey 2002; Gernandt et al. 2008, 2018; Smith et al. 2017). This unique collection is remarkable for the number of specimens of each species that were collected, which provides an opportunity to explore quantitatively the variability of individual characters and discuss the validity of fossil species.

This report represents the first part of the revision of this entire collection from the Belgian Lower Cretaceous. Here we focus on one of the most abundant *Pityostrobus* species found in this collection: *Pityostrobus andraei* (Coemans) Seward 1919. Its intraspecific morphological disparity has been reassessed, and it has been compared with other *Pityostrobus* species. As a result, eight different morphotypes are recognized.

## Material and Methods

### Localities

Studied fossils were collected from two closely located Belgian localities: La Louvière and Houdeng-Aimeries (fig. 1). The first

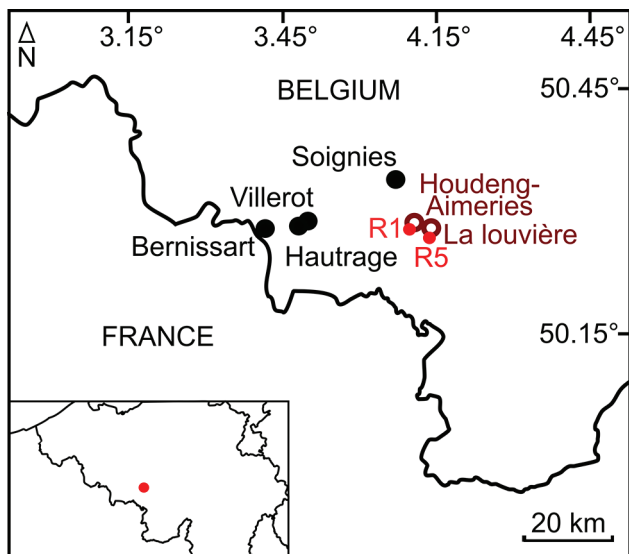


**Fig. 1** Geographical map showing the localities of La Louvière and Houdeng-Aimeries (Roeulx 1 [R1] and Roeulx 5 [R5]), Belgium.

collection was built by Coemans (1867) from a now-abandoned clay quarry in the former hamlet of Baume in La Louvière. The collection was further increased by C. Bommer, who in 1892 collected abundant plant specimens during the construction of floodgate 3 of the “canal du centre” (Bommer 1892; Alvin 1953). These localities are currently not accessible.

Both La Louvière and Houdeng-Aimeries are situated at the eastern limit of the Mons Basin. This basin is part of the Anglo-Paris Basin, representing its northeast rim. The Mons Basin constitutes a 40-km-long and 10-km-wide subsiding zone that accumulated 300 m of Meso-Cenozoic sediments (Yans 2007; Yans et al. 2010). The Wealden facies is exposed as “pockets” at the north of the Mons Basin. They correspond to Cretaceous continental siliciclastic sediments deposited in deltaic complexes. Highly diachronic across the basin, they range in age from middle Barremian (127.3 Ma) in the west to middle-late Albian (100.5 Ma) in the east (Yans et al. 2006; Dejax et al. 2007, 2008; Robaszynski et al. 2007; Gernandt et al. 2008). Although this west-east Barremian–Albian age gradient is supported by some data, several eastern localities of the Wealden facies—Soignies, Houdeng-Aimeries (Roeulx 5), and La Louvière (Roeulx 1)—have never been precisely dated.

### Material

All ovulate cones were found isolated in a sandy clay matrix in association with leaves, twigs, and wood fragments, which were not collected (Bommer 1892). They were mechanically extracted and were not chemically prepared. The cones are lignitized (Alvin 1953, 1971, 1974) and preserve most of their original tridimensional shape, being only slightly compressed. Anatomy and tissues are well preserved (Alvin 1953).

In Belgium, the Wealden facies occurs in five formations: the Hautrage, Baudour, and Sainte-Barbe Formations to the west and the Saint Pierre and Strepy Formations to the east. The layers of La Louvière and Houdeng-Aimeries from which the ovulate cones were collected belong to the Saint-Pierre Formation. Although the two localities were not precisely dated, the Saint-Pierre Formation is dated to the upper half of the Albian (Yans 2007). Precise dating of these localities will be useful for comparisons among the different fossil assemblages of the Mons Basin.

### Sampling

In this study, a sample of 295 complete or incomplete fossil ovulate cones hosted in the RBINS collections was observed. This sampling represents all cones attributed to the species *Pityostrobus andraei* available in the collections. The cone specimens were initially identified as *Pinus andraei* Coemans 1867 by C. Bommer (1892). They were subsequently reinterpreted as *Pityostrobus andraei* (Coemans) Seward 1919 by Alvin (1953). A subsample of 124 of these cones was selected for morphometric analyses because they were either complete or in good condition. The remaining 171 specimens are too fragmented or poorly preserved to be confidently included in one morphotype and to allow for morphometric analysis, as their incompleteness might distort the morphospaces. In addition, eight specimens representing other species of Belgian Pinaceae were incorporated in our analyses to calibrate the amount of morphological variation within *P. andraei*.

as currently defined. These were *Pityostrobus bommeri* Alvin 1953 ( $n = 2$ ), *Pityostrobus haurageanus* Alvin 1960 ( $n = 1$ ), *Pityostrobus soigniesiensis* Alvin 1960 ( $n = 1$ ), *Pityostrobus villetotensis* Alvin 1957 ( $n = 2$ ), *Pseudoaraucaria gibbosa* Alvin 1960 ( $n = 1$ ), and *Pseudoaraucaria heeri* Alvin 1957 ( $n = 1$ ).

#### Imaging and Measurements

First, the selected ovulate cones were classified into several morphotypes based on their general shape and anatomy (see descriptions below). All the specimens selected ( $n = 132$ ) were individually photographed with a Nikon D90 camera equipped with an AF-S DX NIKKOR 18–105mm f/3.5–5.6G ED VR. The photographs were used for bidimensional analysis using linear morphometry. Ten measurements were taken to characterize cone shape, following the protocols of Gil et al. (2002) and Marcysiak (2004), as follows: (1) cone length, (2) width of the cone base, (3) maximal cone width, (4) cone diameter midway between the base and the maximum diameter, (5) width of the scale apophysis in the middle of the cone, (6) height of the scale apophysis in the middle of the cone, (7) angle of the apophysis, (8) length of the cone base (portion that bears reduced scales), (9) number of scales, and (10) number of gyres along an orthostichy (fig. 2; app. A1; apps. A1–A5 are available online). These last two measurements (9 and 10) are subject to a preservation bias because the base and/or the apex was missing on many cones. Therefore, the number of scales and gyres was, whenever possible, extrapolated by means of the scale bases when they were still present or by doubling the number of scales counted on one side of the cone.

Measurements and observations were performed digitally with ImageJ/Fiji 1.52n software (Schindelin et al. 2012; Schneider et al. 2012). For tridimensional observations and anatomical measurements, two cones were scanned at the micro-computed tomography (CT) facility of the RBINS using an EasyTom 150-kV scanner (RX Solutions, 3D X-Ray tomography systems) fitted with a microfocus X-ray source and a 320 × 420-mm detector. Specimens Pbot-0-0231 and IRSNB\_b\_6840 of the RBINS collections (app. A1) were scanned in their entirety using a copper filter. Pbot-0-0231 was scanned at a spatial resolution of 0.019 mm, with an electron acceleration energy of 149 kV and a current of 67  $\mu$ A. IRSNB\_b\_6840 was scanned at a spatial resolution of 0.026 mm, with an electron acceleration energy of 143 kV and a current of 70  $\mu$ A. Scans were used for anatomical descriptions and measurements that were also performed digitally with the ImageJ2 software (Schneider et al. 2012; Rueden et al. 2017). Scans can be consulted on request to the RBINS curator of Palaeontology Collections.

#### Statistical Analyses

To characterize the morphological variability of *P. andraei*, univariate and multivariate tests were applied to the measurements within the R 3.6.0 environment (R Core Team 2019) using the data matrix obtained with the measurements of the bidimensional analysis (fig. 2). For the univariate analysis, the R package readxl version 1.3.1 was used to import the data (Wickham and Bryan 2019). To compare the different morphotypes described, the variables measured are compared with each other to determine whether populations are significantly different.

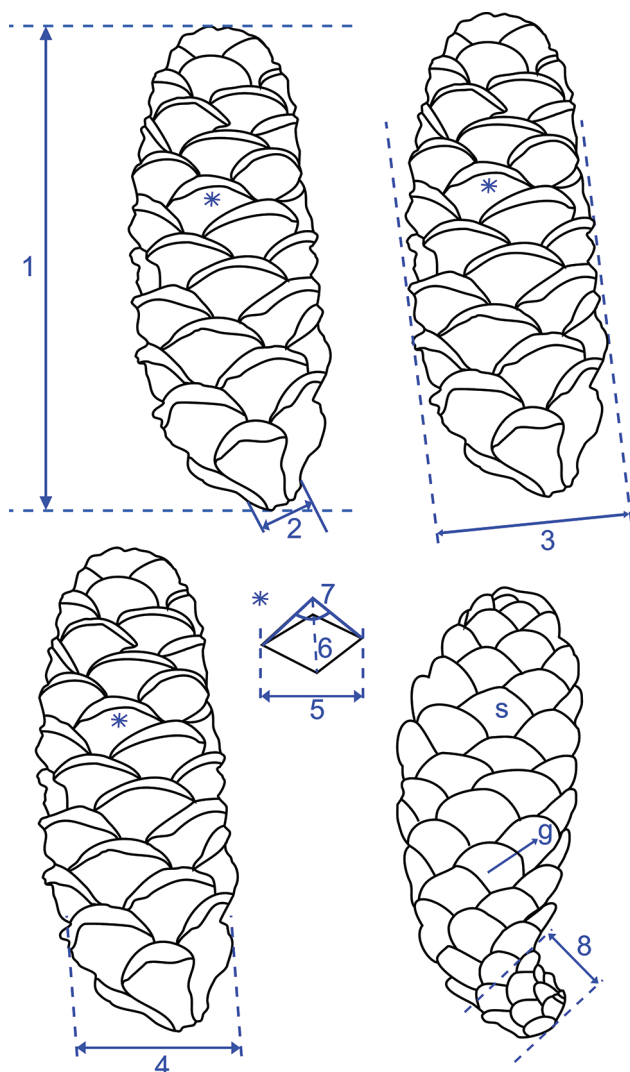


**Fig. 2** Illustration of the eight measurements applied to the ovulate cones, as follows (following Gil et al. 2002; Marcysiak 2004): (1) cone length, (2) length of the cone base, (3) maximal cone width, (4) cone diameter midway between the base and the maximum diameter, (5) width of the scale apophysis in the middle of the cone, (6) height of the scale apophysis in the middle of the cone, (7) angle of the apophysis, and (8) base length (at the bottom of the cone, where the scales are reduced). s = scale; g = gyre.

We tested the normality of selected variables (1, 3, 5, 6, 9, 10; fig. 2) using the Shapiro-Wilk test (Shapiro and Wilk 1965). A Fisher test was applied to test homoscedasticity (Fisher 2006). For testing homogeneity between means of different variables, a parametric Student's *t*-test was performed on data that follow a normal distribution; the nonparametric Wilcoxon test (Mann-Whitney *U*-test) was performed on the others (Wilcoxon 1945; Mann and Whitney 1947). To compare means for variables with homogeneous variances, we used a permutation Student's *t*-test with the R package RVAideMemoire version 0.9-75 (Hervé 2019; app. A2).

Multivariate analysis was performed to characterize the morphospace occupancy of the samples and to circumscribe the different cone morphotypes. The R packages readxl version 1.3.1, ape version 5.3, devtools version 2.3.0, ggplot2 version 3.3.0, and ggbiplot version 0.55 were used (Vu 2011; Wickham 2016; Paradis and Schliep 2019; Wickham and Bryan 2019; Wickham et al. 2020). The data set was scaled ( $z$  transformed), and all individuals with missing data were removed, which produced a matrix of 81 specimens and 12 groups (app. A3). Principal component analysis (PCA) was applied to the resulting data set to circumscribe morphospace occupation. Only seven of the measurements (cone length [1], maximal cone width [3], cone diameter midway between the base and the maximum diameter [4], width of the scale apophysis in the middle of the cone [5], height of the scale apophysis in the middle of the cone [6], scale number [9], and number of gyres along an orthostichy [10]) are included in the PCA because the other measurements have too many missing data to be correctly represented. Morphotypes C, F, and I and the Belgian species *P. gibbosa* are not represented because they are each represented by only one specimen that is missing some data. Normal data ellipses with a size of 0.68 are used to highlight morphospaces for morphotypes with more than two specimens. A multivariate analysis of variance (MANOVA) was computed to test the differences between individuals of morphotypes A and B included in the PCA (Bray et al. 1985). Other morphotypes were removed from the analysis, as they do not have enough specimens.

## Results

### Definition of Morphotypes

Description of the 124 selected cones resulted in the separation of eight morphotypes (fig. 3; table 1). Those specimens either were initially figured by Alvin (1953) as *Pityostrobus andraei* (A, B, G, H) or were classified as *P. andraei* by Alvin in the RBINS collections (C–F). We figured the most representative and relevant cones for each morphotype (fig. 3). Of these specimens, 50% and 25% belong to two morphotypes, referred to as A ( $n = 66$ ) and B ( $n = 30$ ), respectively. Seven percent belong to six other morphotypes, referred to as C–H ( $n = 9$ ; fig. 3; table 1). The remaining 15% of the specimens were not assigned to any morphotype because they were too abraded ( $n = 19$ ; app. A1).

All morphotypes are lignified ovulate cones with bract-scale complexes that are helically arranged. The scales bear two inverted seeds at their base. Seeds are winged.

**Morphotype A.** Morphotype A is represented by lignified ovulate cones that are at least 2.8–7.4 cm long and 1.3–3.2 cm in diameter and ovoid ( $n = 66$ ; 50%; figs. 3A, 4A–4C; IRSNB\_b\_6844). Bract-scale complexes are helically arranged. The ovuliferous scales are 12–20 mm long and 2.6–8 mm wide, oriented at an angle of 20° to the stele axis. Pith is 0.8–1.6 mm in diameter. The vascular cylinder is 150  $\mu\text{m}$  in diameter, slightly dissected, with rare resin canals. Cortex is 0.85–1.4 mm in diameter, with one to five resin canals. Vascular traces to the ovuliferous scale and bract diverge separately from the cone axis; the ovuliferous scale trace is formed from one vascular strand, abaxially concave. Bracts are reduced, 10%–20% of scales' length. There are two seeds per scale, winged, measuring 3.3 mm in length and 1 mm in thickness. Wings measure

two-thirds of the scale length. Sarcotesta and sclerotesta together measure 0.13–0.2 mm.

**Morphotype B.** Morphotype B is represented by lignified ovulate cones that are 7.2–14 cm long and 1.6–3.0 cm in diameter and elongated and cylindrical ( $n = 30$ ; 25%; figs. 3B, 4D–4F; IRSNB\_b\_6840). Bract-scale complexes are helically arranged. The ovuliferous scales are 20 mm long and 6.8–8.5 mm wide, oriented at an angle of 14° to the stele axis. Pith is 1.8–2.1 mm in diameter; resin canals are absent. The vascular cylinder is continuous, slightly dissected at the scale bases, and 0.3–0.4 mm in thickness. Cortex is 0.9–2 mm in diameter, with 15 resin canals. Scale trace is flat at its divergence from the axis and then becomes cylindrical. Apophysis is rhomboid in shape with a terminal umbo. Seeds are ovate in shape and measure, on average, 4.5 mm in length and 1.5 mm in thickness. Sarcotesta and sclerotesta together are 0.15–0.19 mm wide.

**Morphotype C.** Morphotype C is represented by a lignified ovulate cone that is 3.3 cm long and 1.8 cm wide and ovoid cylindrical in shape ( $n = 1$ ; 0.8%; fig. 3C; Pbot-06058-0117). Bract-scale complexes are helically arranged. Ovuliferous scales are 12 mm long and 10 mm wide. Apophysis is flabellate, radially striated, thin, without an umbo. Apophyses are 2.4 mm long and 10 mm in diameter. Scales have two inverted seeds at their base. Seeds are winged and are 2–3.2 mm long and 1.6–1.8 mm in thickness. The sarcotesta and sclerotesta are 0.59 mm thick.

**Morphotype D.** Morphotype D is represented by lignified ovulate cones that are 4.2–4.3 cm long and 2–2.2 cm wide and ovoid in shape ( $n = 2$ ; 1.6%; fig. 3D; Pbot-06058-92). Bract-scale complexes are helically arranged. Ovuliferous scales are 14–15 mm long, 6–9 mm wide, and 0.3–0.8 mm thick. Scales are thickened into a rhomboid apophysis and have no umbo. Apophyses are 7.8–9.4 mm long and 5.4–5.8 mm high. Scales have two inverted seeds at their base. Seeds are winged and are 5–6 mm long and 8–9 mm in thickness. The sarcotesta and sclerotesta are 0.16–0.21 mm thick.

**Morphotype E.** Morphotype E is represented by lignified ovulate cones that are 4.4 cm long and 1.8–2 cm in diameter and elongated and cylindrical in shape ( $n = 3$ ; 2.4%; fig. 3E; Pbot-0-0232). Bract-scale complexes are helically arranged. Scales are thickened into an apophysis, rhomboid and mucronate. Apophyses are 6–7 mm long and 8–9 mm wide. A terminal umbo is present and follows the shape of the apophysis.

**Morphotype F.** Morphotype F is represented by a lignified ovulate cone that is 6 cm long and 3.1 cm wide and ovoid and cylindrical in shape ( $n = 1$ ; 0.8%; fig. 3F; Pbot-0-0160). Bract-scale complexes are helically arranged. Ovuliferous scales are 20 mm long and 8–10 mm wide. Reduced bracts are visible. Scales are distally thickened and slightly folded abaxially, forming a rhomboid-mucronate apophysis. Apophyses are 6.3 mm long, 10 mm wide, and 1.5 mm thick. Scales have two inverted seeds at their base. Seeds are winged. The sarcotesta and sclerotesta are 0.16 mm thick.

**Morphotype G.** Morphotype G is represented by a lignified ovulate cone that is 5.9 cm long and 2.1 cm wide and cylindrical in shape ( $n = 1$ ; 0.8%; fig. 3G; IRSNB\_b\_6855). Bract-scale complexes are helically arranged. Ovuliferous scales are 16 mm long, 6–9 mm wide, and 0.5–1 mm thick. Scales are distally thickened, forming a rounded apophysis. Apophyses are 7.7 mm long and 11 mm wide and have a terminal umbo folded abaxially. Scales have two inverted seeds at their base. Seeds are winged

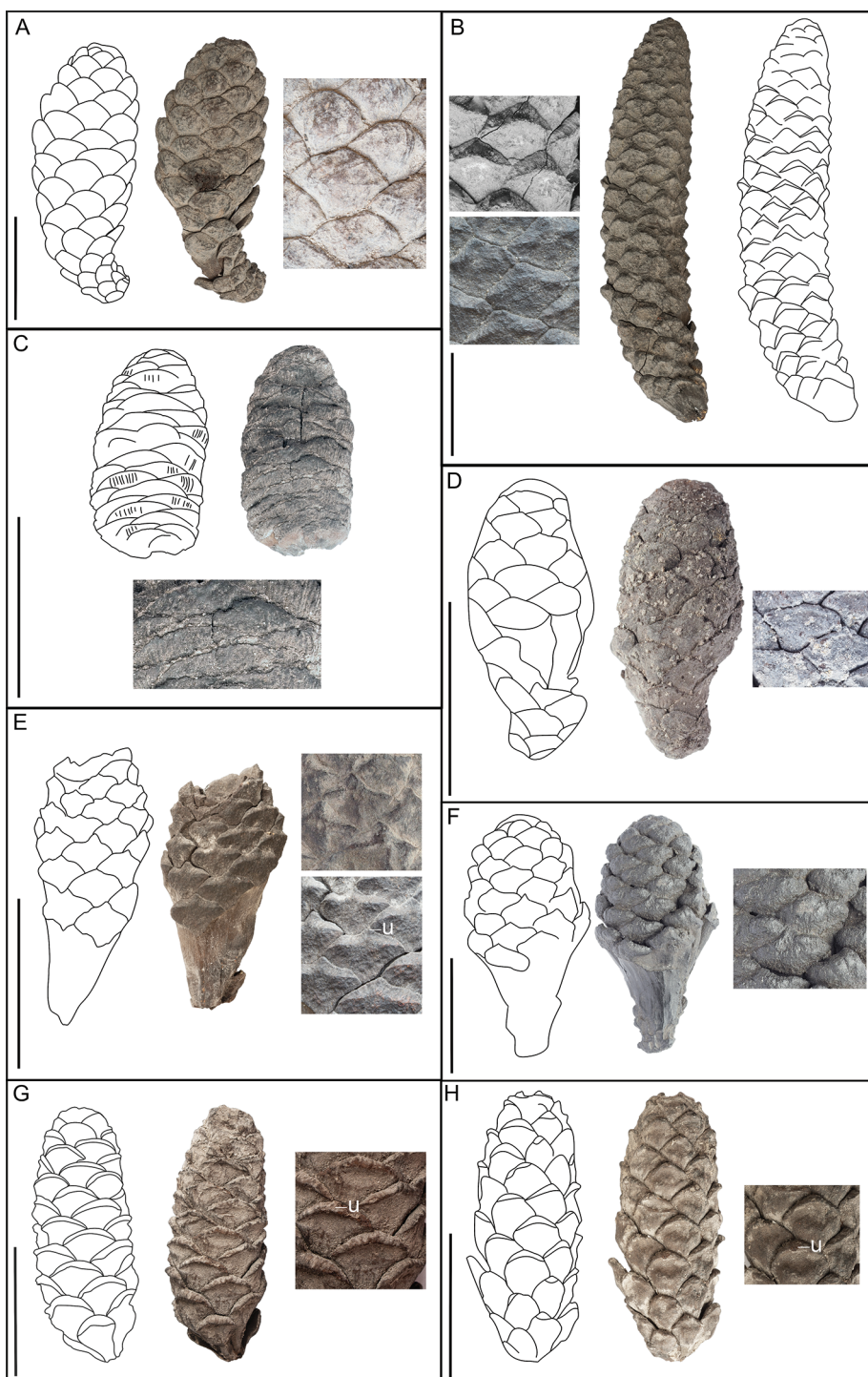


**Fig. 3** Eight morphotypes separated within the sample ( $n = 124$ ) of *Pityostrobus andraei* species. A, Morphotype A, IRSNB\_b\_6844; 50%. B, Morphotype B, IRSNB\_b\_6840; 25%. C, Morphotype C, Pbot-06058-0117; interpreted as close to *Pityostrobus villerotensis*. D, Morphotype D, Pbot-06058-92. E, Morphotype E, Pbot-0-0232; submature stage of morphotype B. F, Morphotype F, Pbot-0-0160. G, Morphotype G, IRSNB\_b\_6855. H, Morphotype H, IRSNB\_b\_6843. Scale bars = 3 cm. u = umbo.

and are 4.8 mm long and 1.9–2.2 mm in diameter. The sarcotesta and sclerotesta are 0.1 mm thick.

*Morphotype H.* Morphotype H is represented by a lignified ovulate cone that is 5.5 cm long and 2 cm wide and cylindrical

in shape ( $n = 1$ ; 0.8%; fig. 3H; IRSNB\_b\_6843). Bract-scale complexes are helically arranged. Scales are distally thickened, forming an acute apophysis. Apophyses are 9 mm long and 9.2 mm wide and have a terminal umbo that is slightly folded

**Table 1**  
**Comparison of the Main Characteristics of the Eight Morphotypes**

Morphotype	<i>n</i>	Sample percentage (%)	General features			Cone axis		
			Cone shape	Cone length (mm)	Cone width (mm)	Pith diameter (mm)	Vascular cylinder diameter (mm)	Cortex diameter (mm)
A	66	50	Ovoid	28–74	13–32	.8–1.6	.15	.85–1.4
B	30	25	Elongated and cylindrical	72–140	16–30	1.8–2.1	.3–4	.9–2
C	1	.8	Ovoid and cylindrical	33	18	na	na	na
D	2	1.6	Ovoid	42	20	1.7–2	na	na
E	3	2.4	Elongated and cylindrical	44	18–20	na	na	na
F	1	.8	Ovoid and cylindrical	60	31	na	na	na
G	1	.8	Cylindrical	59	21	na	na	na
H	1	.8	Cylindrical	55	20	na	na	na
Ovuliferous scales			Apophysis			Seeds		
Resin canals in the cortex	Length (mm)	Width (mm)	Umbo absence/presence and position	Length (mm)	Width (mm)	Sarcotesta and sclerotesta thickness (mm)	Length (mm)	Width (mm)
A	1–5	12–20	2.6–8	Not present	3.6–10	.5–13	.13–2	3.3
B	15	20	6.8–8.5	Terminal	8.4	7.6	.15–19	4.5
C	na	na	10	Not present	2.4	10	.59	2–3.2
D	na	na	6–9	Not present	7.8–9.4	5.4–5.8	.16–21	5–6
E	na	na	na	Terminal	6–7	8–9	na	na
F	na	20	8–10	Not present	6.3	10	.16	na
G	na	16	6–9	Terminal	7.7	11	.1	4.8
H	na	na	9.2	Terminal	9	9.2	na	na

Note. The table is based on 586 measurements in millimeters. na = not applicable.

abaxially. Scales have two inverted seeds at their base. Seeds are winged.

#### Morphometric Analyses

Our data set scores 10 variables for 132 specimens. Although the data set has a fairly low proportion of missing data (32%; app. A1), the completeness threshold for our multivariate analyses required a data set reduction to seven variables for 81 specimens (0% missing data).

Because of this, only morphotypes A and B are amenable to statistical comparison. We thus here focus on the characterization and the comparison of their respective variabilities. Morphotypes C–H are excluded from these analyses as they are represented by only one to three specimens each (0.8%–2.4% of the sample). Half of these specimens have missing data because of distortion or poor preservation.

#### Univariate Analysis

The results of this analysis are presented in five boxplots comparing the cones in terms of length (variable 1), the cone length-to-width ratio (1, 2), the apophysis shape ratio (width-to-height; 5, 6), the number of scales (9), and the number of gyres (10), along with the associated *P* values (fig. 5; app. A4).

These characters were chosen because they are the most representative variables describing cone morphology with the least missing data.

Continuous variables measured for morphotypes A and B are distributed on significantly different intervals (see *P* values; fig. 5). Cone length differs significantly between morphotypes A and B (fig. 5.1; Student's *t*-test: *P* < 0.0001). The cone length-to-width ratio is also significantly different between the two morphotypes (fig. 5.2; Student's *t*-test: *P* < 0.0001). The difference in apophysis size is also significant (fig. 5.3; Student's *t*-test: *P* < 0.0001). The apophysis shape ratio of morphotype A is much more variable than that of morphotype B (from 0.89 to 2.05 vs. from 0.83 to 1.5, respectively; *P* < 0.01; app. A2). The number of scales (fig. 5.4; permutation Student's *t*-test: *P* = 0.002) and number of gyres (fig. 5.5; Wilcoxon test: *P* < 0.0001) are significantly different as well: morphotype B has more scales and gyres than morphotype A.

Morphotypes C–H were not included in this univariate analysis. The low number of individuals did not allow us to perform statistical tests. However, the visualization of the individuals in the boxplots allowed us to see that morphotypes D–H have values close to those of morphotypes A and B (app. A5). Only morphotype C shows an extreme value for the apophysis shape ratio. This is explained by its scales, which are very

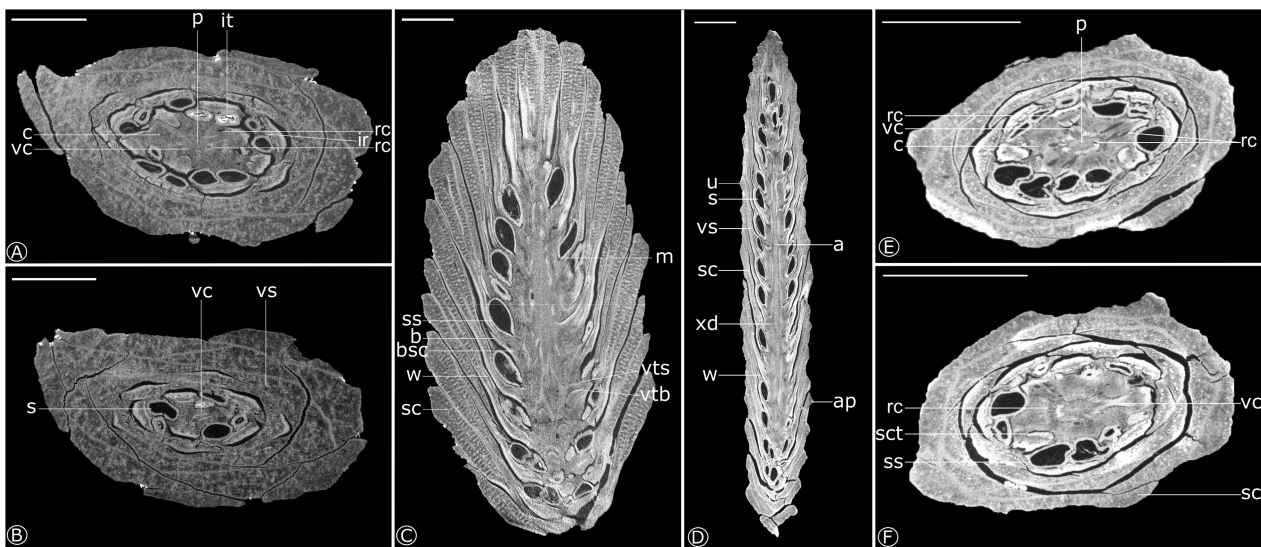


**Fig. 4** Internal views of morphotype A (A–C; Pbot-0-0231; spatial resolution of 0.019 mm, 149 kV, 67  $\mu$ A) and morphotype B (D–F; IRSNB\_b\_6840; spatial resolution of 0.026 mm, 143 kV, 70  $\mu$ A). A, B, E, and F are transverse sections; C and D are longitudinal sections. A, Vascular cylinder with rare resin canals, cortex with one to five resin canals, and two seeds per scale. B, Slightly dissected vascular cylinder; the ovuliferous scale trace is formed from one vascular strand. C, Ovuliferous scale is oriented at an angle of 20° to the stipe axis, vascular traces to the ovuliferous scale and bract diverge separately from the cone axis, and bracts are reduced, 10%–20% of scales' length. D, Ovuliferous scales are oriented at an angle of 14° to the stipe axis. E, Resin canals are absent from the pith, the cortex has 15 resin canals, and the scale trace is flat on derivation of the axis and then becomes cylindrical. F, Vascular cylinder is continuous and slightly dissected at the scale bases. Scale bars = 1 cm. a = axis; ap = apophysis; b = bract; bsc = bract-scale complex; c = cortex; ir = interseminal ridge; it = internal tissue; m = micropyle; p = pith; rc = resin canal; s = seed; sc = scale; sct = scale trace; ss = sarcotesta and sclerotesta; u = umbo; vc = vascular cylinder; vs = vascular strand; vt = bract vascular trace; vts = scale vascular trace; w = wing; xd = xylem discontinuity.

large and flat compared with those of the other morphotypes (fig. 3).

#### Multivariate Analysis

The measurements were analyzed by means of a PCA to observe the distribution of the different morphotypes in different morphospaces (fig. 6; app. A4). Morphotypes A and B are included in the analysis. The MANOVA shows that the specimens of morphotypes A and B included in the multivariate analysis are significantly different ( $P < 0.0001$ ).

Components 1 and 2 represent 53.2% and 19.8% of the total measured variance, respectively. Component 1 is mainly influenced by the length and the middiameter (−0.42 and 0.4, respectively). After that, apophysis width (−0.375), apophysis length (−0.385), apophysis height (−0.345), number of scales (−0.381), and number of gyres (−0.332) all equally influence component 1. Component 2 is mostly influenced by the number of gyres and cone width (0.585 and −0.457, respectively). Morphotypes A and B occupy two distinct morphospace regions that are only slightly overlapping. The specimens attributed to morphotype A are more dispersed than those attributed to morphotype B. Morphotypes C and F are not represented in the PCA because they were removed in response to the completeness threshold. Morphotypes E and H are located in the same morphospace region as morphotype B, while morphotypes D, G, and H are located in the same region as morphotype A. The *Pseudoaraucaria heeri* specimen is also located in the same

morphospace as morphotype A. The specimens of *Pityostrobus bommeri*, *Pityostrobus haurageanus*, *Pityostrobus soigniesiensis*, and *Pityostrobus villerotensis* are isolated apart from the morphotype A and B morphospaces. The nine unidentified specimens are all located within or in proximity to the morphospace of morphotype A.

#### Discussion

##### Species Delimitation in *Pityostrobus*

Our results allow us to reconsider the species concept of *Pityostrobus andraei* in light of the amount of morphological disparity that it encompasses. When Coemans (1867) and then Alvin (1953) first described the specimens, they assigned the 303 specimens of the RBINS collections to *Pinus andraei* Coemans 1866 and then to *Pityostrobus andraei* (Coemans) Seward 1919, respectively. Among these specimens, we were able to differentiate eight morphotypes, of which morphotypes A and B are the most abundant.

The results of the univariate statistical analysis strongly support the hypothesis that morphotypes A and B (fig. 5) represent two distinct species. The use of continuous characters allows us to significantly differentiate the two morphotypes (see  $P$  values; fig. 5). Measurements were made of the external morphology of the cones (fig. 2; app. A1), although these external features are not clearly defined as diagnostic at the species level in existing descriptions (Miller 1976). Here, they allow us to quantify and to render the descriptions mutually consistent. Cone

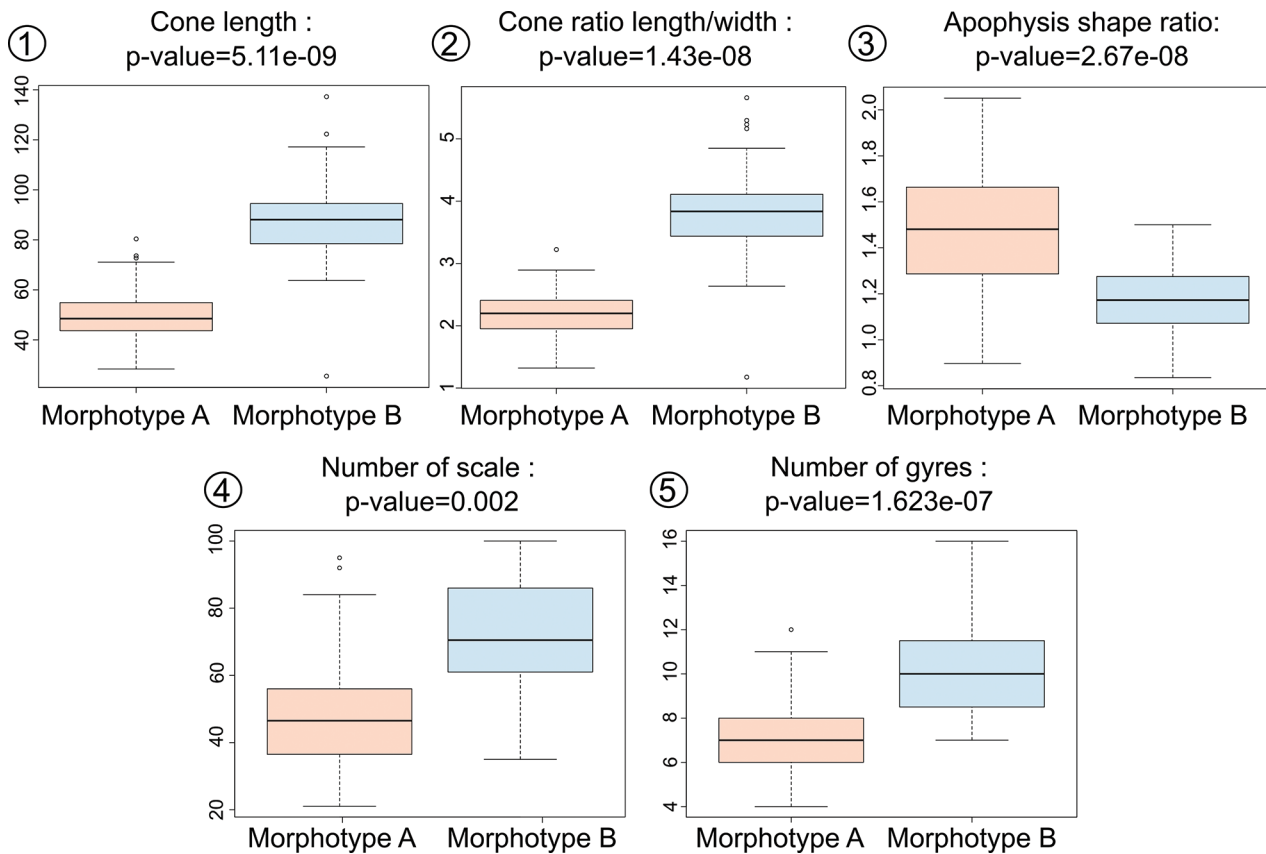


**Fig. 5** Boxplots representing morphometric comparison between morphotypes A and B, including specimens with missing data. Morphotype A:  $n = 66$ ; morphotype B:  $n = 30$ . 1, Cone length. 2, Cone length-to-width ratio. 3, Apophysis shape ratio. 4, Number of scales. 5, Number of gyres.

length and width, apophysis width and height, and number of scales and gyres are all significantly different between the two morphotypes (fig. 5).

Morphotype C looks very similar to the species *Pityostrobus villerotensis* in ovoid-cylindrical shape; thin, flabellate, radially striated apophysis; lack of an umbo; and the sclerotesta and sarcotesta measuring 0.59 mm in diameter. However, *P. villerotensis* was found in a different locality (Villerot) than the cone included in our analyses; Villerot, like the La Louvière and Houdeng-Aimeries localities, has not been dated yet (fig. 1). On the other hand, the Villerot locality is located farther west in the basin and should be older than La Louvière (Yans et al. 2010). Morphotype C could be younger than but morphologically close to *P. villerotensis*.

The PCA shows that the combination of cone measurements that we used enables the assessment of intraspecific variation and clearly shows that morphotypes A and B occupy different morphological spaces. There is no gradual transition from the space occupied by one of the morphospaces to the other, and the overlap between the two morphospaces is minute.

Although morphotypes A and B both include ovulate cones with scales that thicken into an apophysis at the apex and bear two inverted seeds adaxially at their base, figures 5 and 6 highlight the many differences between these two morphotypes. Ad-

ditional differences can be listed as follows: (1) the bract, which is clearly visible in morphotype A, is not visible in morphotype B, (2) the scale base is thinner in morphotype A, (3) the secondary xylem of the axis is more dissected in morphotype A, (4) the shape of the scale trace is flat in morphotype B and abaxially concave in morphotype A, and (5) cortical resin canals are more numerous in morphotype B.

Coemans (1867) and Alvin (1953) were both aware of its great variability when they described *P. andraei*. Alvin (1953) justified the inclusion of the morphotypes defined here in the same species based on their consistent association in the two localities. As some cones were a little abraded on the surface, he interpreted those that we include in morphotype A as representing either an immature stage or very abraded specimens of *P. andraei* (morphotype B). Here, we show that although some cones of morphotype A were abraded, most of them are well preserved (both internal and external structures). Furthermore, both morphotypes comprise mature or submature specimens, as they are completely lignified, have reduced bracts, and bear mature seeds.

In our opinion, the results of the morphometric analysis, combined with the other morphological and anatomical differences that we highlighted above (cone shape, scale shape, umbo and bract presence, and scale trace shape; see table 1), should be

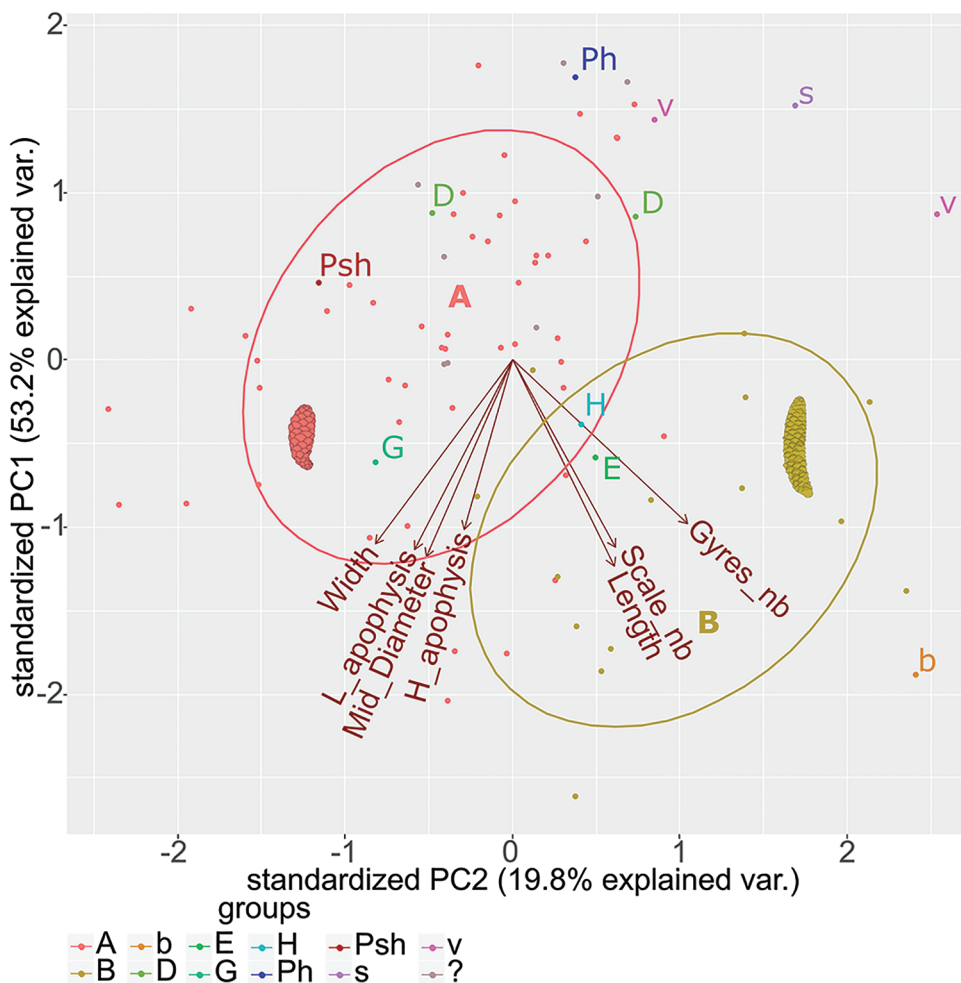


**Fig. 6** Morphospace occupation using the first two axes of the principal components (PC) analysis ( $n = 81$ ) with superimposed 68% confidence ellipses for each group. Multivariate analysis of variance (var.),  $P < 0.0001$ . Length; width; mid\_diameter = cone diameter midway between the base and the maximum diameter; l\_apophysis = width of the scale apophysis; h\_apophysis = height of the scale apophysis; scale\_nb = scale number; gyres\_nb = number of gyres along an orthostichy. Groups: A = morphotype A ( $n = 48$ ); B = morphotype B ( $n = 14$ ); b = *Pityostrobus bommeri* ( $n = 1$ ); D = morphotype D ( $n = 1$ ); E = morphotype E ( $n = 1$ ); G = morphotype G ( $n = 1$ ); H = morphotype H ( $n = 1$ ); Ph = *Pityostrobus hautrageanus* ( $n = 1$ ); Psh = *Pseudoaraucaria heeri* ( $n = 1$ ); s = *Pityostrobus soigniesiensis* ( $n = 1$ ); v = *Pityostrobus villerotensis* ( $n = 2$ ); ? = undetermined morphotype ( $n = 9$ ).

enough to justify splitting *P. andraei* into at least two distinct species (corresponding to our morphotypes A and B). To redefine the species concept of *P. andraei* in the absence of a clearly defined holotype, isotype, isosyntype, or syntype, a lectotype must be selected from among the illustrated specimens (Turland et al. 2018, chap. II, art. 9.3). This formal taxonomic decision will be the subject of a separate upcoming article. As these Belgian species are included in recent studies on the evolution of Pinaceae (Gernhardt et al. 2016; Smith et al. 2017), these new systematic data will probably bring new information to the phylogenies.

#### Morphometry-Informed Taxonomic Diversity among Fossil Cones

Pinaceous cones are structures that are rarely preserved compared with the vegetative parts of conifers. They are also more

likely to disarticulate before burial. This explains why most Cretaceous ovulate cone descriptions are based on isolated or incomplete specimens (Gernhardt et al. 2016; table 1). It is also common for external features of the cone to be difficult to observe (e.g., cones encased in nodules; Falder et al. 1998; Rothwell et al. 2012). This is compounded by the fact that many cone morphospecies were described more than 50 years ago (Alvin 1953, 1957, 1960), when species concepts were somewhat different from those employed nowadays. As a result, the taxonomy of fossil Pinaceae is at times inconsistent (Miller 1976; Ryberg et al. 2012; Smith et al. 2017), and this distorts our understanding of the assembly of their diversity throughout the Mesozoic and the Cenozoic. Yet conifer reproductive structures are an ideal organ to study in a comparative framework because they possess many diagnostic characters, which are commonly employed to define fossil and extant species (Farjon 2005).

Our approach is aimed at homogenizing descriptions and taxonomy within a thorough comparative framework and constitutes a first step in the use of morphometrics to study the diversity of pinaceous cones. This type of approach was already tested on extant Pinaceae species in three studies on cone morphology (Gil et al. 2002; Marcysiak 2004; Vetrova 2013). On the other hand, studies of fossil species have already been conducted with other plant groups using morphometric data (Roth-Nebelsick et al. 2000; Benca et al. 2014) but not with Pinaceae species.

The next step will be to apply this methodology to all the different morphotaxa of Belgian fossil ovulate cones from the Cretaceous that are represented by enough specimens to assess their intra- and interspecific variability (Herrera et al. 2015, 2017). Eventually, this will provide important data to complement the studies already carried out on the disparity of conifer cones (Leslie 2011; Smith et al. 2017). The analysis of continuous characters opens the way for accurate disparity studies through the use of linear and geometric morphometrics, which has rarely been used, up until now, with plants (Oyston et al. 2016).

### Conclusions

Descriptions of pinaceous morphotaxa are subject to several inherent biases: quality of preservation, number of fossilized specimens, and subjectivity of identification, depending on the author. A combination of descriptions and quantitative analyses is applied to homogenize the identifications. The aim is to establish a methodology for reproducible analyses of individuals of the same family.

By applying morphometrics to a large sample of ovulate cones ( $n = 132$ ), we were able to clearly distinguish two different morphotypes included in the species *Pityostrobus andraei* (A and B). The use of descriptions combined with statistical analyses demonstrates that morphotypes A and B belong to two distinct populations. We quantify the cone morphology (length, width,

apophysis shape, number of cone scales and gyres). Statistical analyses demonstrate that these features are significantly different between morphotypes A and B (fig. 5). The PCA shows that the combination of measurements of multiple features of the cone morphology enables the assessment of interspecies variation. The PCA clearly shows that morphotypes A and B occupy different morphospace regions. The main differences are cone shape, scale shape, the length of the bract in morphotype A, the number of resin canals in the cortex, and the sclerotesta and sarcotesta thickness.

This work shows that the specific diversity of the ovulate cones found in the Belgian Lower Cretaceous (Wealden facies) needs to be reevaluated, as the species concept of *P. andraei* initially described by Alvin (1953) includes clearly distinct morphotypes that should be elevated to morphospecies. These morphotypes make it possible to reassess the number of known species in Belgium and consequently Pinaceae diversity during the Early Cretaceous.

Future work should clarify systematics problems for fossil species currently classified within the genera *Pinus* and *Pityostrobus*. Combining this with a review of the Belgian fossil species will allow further characterization of the diversity of the Pinaceae during a key period of their evolution.

### Acknowledgments

The specimens were scanned by Dr. Ulysse Lefevre using the RX EasyTom of the RBINS micro-CT facility in the framework of the DiSSCo-Fed project (coordinator, Dr. Patrick Semal) of the Belgian Federal Science Policy. The work of L. De Brito is supported by a FRIA grant from the FRS-FNRS (grant FC 31575). We thank Dr. V. Fischer and Dr. J. Goedert for their readings as well as Andrew Leslie and an anonymous reviewer for their valuable comments, which greatly helped to improve the manuscript.

### Literature Cited

- Alvin KL 1953 Three abietaceous cones from the Wealden of Belgium. Inst R Sci Nat Belg Mem 125:1–42.
- 1957 On the two cones *Pseudoaraucaria heeri* (Coemans) nov. comb. and *Pityostrobus villerotensis* nov. sp. from the Wealden of Belgium. Inst R Sci Nat Belg Mem 135:1–27.
- 1960 Further conifers of the Pinaceae from the Wealden formation of Belgium. Inst R Sci Nat Belg Mem 146:1–39.
- 1971 *Weichselia reticulata* (Stokes et Webb) Fontaine. Inst R Sci Nat Belg Mem 166:1–33.
- 1974 Leaf anatomy of Weichselia based on fusainized material. Palaeontology 17:587–598.
- Benca JP, MH Carlisle, S Bergen, CAE Strömberg 2014 Applying morphometrics to early land plant systematics: a new Leclercqia (Lycopida) species from Washington State, USA. Am J Bot 101:510–520.
- Bommer C 1892 Un nouveau gîte à végétaux découvert dans l'argile wealdienne de Bracquegnies. Bull Soc Belg Geol 6:160–161.
- Bonnot E-J, H Des Abbayes, M Chadefaud, Y de Ferré, J Feldmann, H Gaussen, P-P Grasse, C Lerédde, P Ozenda, A-R Prévôt 1963 Botanique: anatomie, cycles évolutifs, systématique. Publ Soc Linn Lyon 34:27–29.
- Bray JH, SE Maxwell, SE Maxwell 1985 Multivariate analysis of variance. CS Newbury Park, ed. Sage, London.
- Coemans E 1867 Description de la flore fossile du premier étage du terrain crétacé du Hainaut. Mem Acad R Sci Lett B-arts Belg 36:1.
- Critchfield WB, EL Little 1966 Geographic distribution of the pines of the world. USDA, Forest Service, Washington, DC.
- Dejax J, D Pons, J Yans 2007 Palynology of the dinosaur-bearing Wealden facies in the natural pit of Bernissart (Belgium). Rev Palaeobot Palynol 144:25–38.
- 2008 Palynology of the Wealden facies from Hautrage quarry (Mons Basin, Belgium). Mem Geol Surv 55:45–52.
- Falcon-Lang HJ, V Mages, M Collinson 2016 The oldest *Pinus* and its preservation by fire. Geology 44:303–306.
- Falder AB, GW Rothwell, G Mapes, RH Mapes, LA Doguzhaeva 1998 *Pityostrobus milleri* sp. nov., a pinaceous cone from the Lower Cretaceous (Aptian) of southwestern Russia. Rev Palaeobot Palynol 103:253–261.
- Farjon A 2005 Pines: drawings and descriptions of the genus *Pinus*. Brill, Leiden.
- Fisher RA 2006 Statistical methods for research workers. Genesis, New Dehli.
- Gernandt DS, G Holman, C Campbell, M Parks, S Mathews, LA Raubeson, A Liston, RA Stockey, GW Rothwell 2016 Phylogenetics of extant and fossil Pinaceae: methods for increasing topological stability. Botany 94:863–884.

- Gernandt DS, S Magallón, G Geda López, O Zerón Flores, A Willyard, A Liston 2008 Use of simultaneous analyses to guide fossil-based calibrations of Pinaceae phylogeny. *Int J Plant Sci* 169:1086–1099.
- Gernandt DS, C Reséndiz Arias, T Terrazas, X Aguirre Dugua, A Willyard 2018 Incorporating fossils into the Pinaceae tree of life. *Am J Bot* 105:1329–1344.
- Gil L, J Climent, N Nanos, S Mutke, I Ortiz, G Schiller 2002 Cone morphology variation in *Pinus canariensis* Sm. *Plant Syst Evol* 235:35–51.
- Herrera F, G Shi, P Knopf, AB Leslie, N Ichinnorov, M Takahashi, PR Crane, PS Herendeen 2017 Cupressaceae conifers from the Early Cretaceous of Mongolia. *Int J Plant Sci* 178:19–41.
- Herrera F, G Shi, AB Leslie, P Knopf, N Ichinnorov, M Takahashi, PR Crane, PS Herendeen 2015 A new voltzian seed cone from the Early Cretaceous of Mongolia and its implications for the evolution of ancient conifers. *Int J Plant Sci* 176:791–809.
- Hervé M 2019 RVAideMemoire: testing and plotting procedures for biostatistics. R package version 0.9-73. <http://cran.r-project.org/web/packages/RVAideMemoire/index.html>.
- Klymiuk AA, RA Stockey 2012 A Lower Cretaceous (Valanginian) seed cone provides the earliest fossil record for *Picea* (Pinaceae). *Am J Bot* 99:1069–1082.
- Leslie A 2011 Shifting functional roles and the evolution of conifer pollen-producing and seed-producing cones. *Paleobiology* 37:587–602.
- Mann H, D Whitney 1947 On a test of whether one of two random variables is stochastically larger than the other. *Ann Math Stat* 18:50–60.
- Marcysiak K 2004 Interpopulational variability of *Pinus uncinata* Ramond ex DC. in Lam. & DC. (Pinaceae) cone characters. *Dendrobiology* 51:43–51.
- Miller CN 1976 Early evolution in the Pinaceae. *Rev Palaeobot Palynol* 21:101–117.
- 1977 Mesozoic conifers. *Bot Rev* 43:217–280.
- Oyston JW, M Hughes, S Gerber, MA Wills 2016 Why should we investigate the morphological disparity of plant clades? *Ann Bot* 117:859–879.
- Paradis E, K Schliep 2019 ape 5.0: an environment for modern phylogenetics and evolutionary analyses in R. *Bioinformatics* 35: 526–528.
- R Core Team 2019 R: a language and environment for statistical computing. R Foundation for Statistical Computing, Vienna.
- Robaszynski F, VA Dhondt, JWM Jagt 2007 Cretaceous lithostratigraphic units (Belgium). *Geol Belg* 4:121–134.
- Roth-Nebelsick A, G Grimm, V Mosbrugger, H Hass, H Kerp 2000 Morphometric analysis of *Rhynia* and *Asteroxylon*: testing functional aspects of early land plant evolution. *Paleobiology* 26:405–418.
- Rothwell GW, G Mapes, RA Stockey, J Hilton 2012 The seed cone *Eathiestrobus* gen. nov.: fossil evidence for a Jurassic origin of Pinaceae. *Am J Bot* 99:708–720.
- Rueden CT, J Schindelin, MC Hiner, BE DeZonia, AE Walter, ET Arena, KW Eliceiri 2017 ImageJ2: ImageJ for the next generation of scientific image data. *BMC Bioinformatics* 18:529.
- Ryberg PE, GW Rothwell, RA Stockey, J Hilton, G Mapes, JB Ridling 2012 Reconsidering relationships among stem and crown group Pinaceae: oldest record of the genus *Pinus* from the Early Cretaceous of Yorkshire, United Kingdom. *Int J Plant Sci* 173:917–932.
- Schindelin J, I Arganda-Carreras, E Frise, V Kaynig, M Longair, T Pietzsch, S Preibisch, C Rueden, S Saalfeld, B Schmid 2012 Fiji: an open-source platform for biological-image analysis. *Nat Methods* 9:676–682.
- Schneider CA, WS Rasband, KW Eliceiri 2012 NIH Image to ImageJ: 25 years of image analysis. *Nat Methods* 9:671.
- Seward AC 1919 Fossil plants. Vol 4. Cambridge University Press, Cambridge.
- Shapiro SS, MB Wilk 1965 An analysis of variance test for normality (complete samples). *Biometrika* 52:591–611.
- Smith SY, RA Stockey 2002 Permineralized pine cones from the Cretaceous of Vancouver Island, British Columbia. *Int J Plant Sci* 163: 185–196.
- Smith SY, RA Stockey, GW Rothwell, SA Little 2017 A new species of *Pityostrobus* (Pinaceae) from the Cretaceous of California: moving towards understanding the Cretaceous radiation of Pinaceae. *J Syst Palaeontol* 15:69–81.
- Taylor EL, TN Taylor, M Krings 2009 Paleobotany: the biology and evolution of fossil plants. Academic Press, London.
- Turland NJ, JH Wiersema, FR Barrie, W Greuter, DL Hawksworth, PS Herendeen, S Knapp, W-H Kusber, D-Z Li, K Marhold 2018 International code of nomenclature for algae, fungi, and plants (Shenzhen Code) adopted by the Nineteenth International Botanical Congress Shenzhen, China, July 2017. Koeltz Botanical, Glashütten, Germany.
- Vetrova VP 2013 Geometric morphometric analysis of shape variation in the cone-scales of *Pinus pumila* (Pall.) Regel (Pinaceae) in Kamchatka. *Bot Pac* 2:19–26.
- Vu VQ 2011 ggbioplot: a ggplot2 based biplot. R Package version 0.55.342. <http://www.rdocumentation.org/packages/ggbioplot/versions/0.55.342>.
- Watkins JE, CL Cardelús 2012 Ferns in an angiosperm world: Cretaceous radiation into the epiphytic niche and diversification on the forest floor. *Int J Plant Sci* 173:695–710.
- Wickham H 2016 ggplot2: elegant graphics for data analysis. Springer, Cham, Switzerland.
- Wickham H, J Bryan 2019 readxl: read Excel files. <http://readxl.tidyverse.org/>.
- Wickham H, J Hester, W Chang 2020 devtools: tools to make developing R packages easier. R package version 2.2.2. <https://rdrri.io/cran/devtools/>.
- Wilcoxon F 1945 Individual comparisons by ranking methods. *Biometr Bull* 1:80–83.
- Yans J 2007 Lithostratigraphie, minéralogie et diagenèse des sédiments à faciès wealdien du Bassin de Mons (Belgique). Classe des Sciences, Académie Royale de Belgique, Brussels.
- Yans J, J Dejax, D Pons, L Taverne, P Bultynck 2006 The iguanodonts of Bemissart (Belgium) are middle Barremian to earliest Aptian in age. *Bull Inst R Sci Nat Belg Sci Terre* 76:91–95.
- Yans J, T Gerards, P Gerrienne, P Spagna, J Dejax, J Schnyder, J-Y Storme, E Keppens 2010 Carbon-isotope analysis of fossil wood and dispersed organic matter from the terrestrial Wealden facies of Hautrage (Mons Basin, Belgium). *Palaeogeogr Palaeoclimatol Palaeoecol* 291:85–105.